DTIC COPY

REPORT DOCUMENTATION PAGE

Form Approved
OMB No. 0704-01-0188

PLEASE DO NOT RETURN YOUR FORM TO THE ABOVE ADDRESS.

1. REPORT DATE *(DD-MM-YYYY)*	2. REPORT TYPE	3. DATES COVERED *(From - To)*
24-08-2009	REPRINT	

4. TITLE AND SUBTITLE

Near-infrared collisional radiative model for Xe plasma electrostatic thrusters: the role of metastable atoms

5a. CONTRACT NUMBER

5b. GRANT NUMBER

5c. PROGRAM ELEMENT NUMBER
61102F

6. AUTHORS
Rainer A. Dressler*
Yu-hui Chiu
Oleg Zatsarinny**
Klaus Bartschat**
Rajesh Srivastava#
Lalita Sharma#

5d. PROJECT NUMBER
2303

5e. TASK NUMBER
RS

5f. WORK UNIT NUMBER
A1

7. PERFORMING ORGANIZATION NAME(S) AND ADDRESS(ES)

Air Force Research Laboratory /RVBXT
29 Randolph Road
Hanscom AFB, MA 01731-3010

8. PERFORMING ORGANIZATION REPORT NUMBER
AFRL-RV-HA-TR-2009-1116

9. SPONSORING/MONITORING AGENCY NAME(S) AND ADDRESS(ES)

10. SPONSOR/MONITOR'S ACRONYM(S)
AFRL/RVBXT

11. SPONSOR/MONITOR'S REPORT NUMBER(S)

12. DISTRIBUTION/AVAILABILITY STATEMENT
Approved for Public Release; distribution unlimited.

13. SUPPLEMENTARY NOTES
Reprinted from *Journal of Physics D: Applied Physics*, Vol. **42** (2009) 185203. doi:10.1088/00223727/42/28/185203.
*Spectral Sciences, Inc., 4 Fourth ave., Burlington, MA01803 (continued)

14. ABSTRACT Metastable Xe atoms play an important role in the collisional radiative processes of dense xenon plasmas, including those of electric thrusters for space vehicles. Recent measurements and calculations of electron-excitation processes out of the $5p^5 6s$ J = 2 metastable state ($1s_5$ state in Pas-chen notation) have allowed for the development of a collisional radiative model for Xe near-infrared (NIR) emissions based on the population of the metastable level through $2p\text{-}1s_5$ radiative transitions, and based on depopulation through electron-impact excitation. A modified plasma radi-ative model incorporating newly computed electron-impact excitation cross sections using both relativistic distorted wave and semi-relativistic Breit-Pauli B-Spline R-matrix methods is presented. The model applies to optically thin, low-density regions of the thruster plasma and is most accurate at electron temperatures below 10 eV. The model is tested on laboratory spectral measurements of the D55 TAL and BHT-200 Hall thruster plasma NIR radiation. The metastable neutral fraction is determined to rise from 0.1 to slightly above 1% as the electron temperature increases from ~2 to 10 eV, reaching a maximum around 15 eV. Electron temperatures derived with the modified model are approximately 20% lower than a previous version of the model that used an approximate approach to account for metastable population and line intensity enhancement.

15. SUBJECT TERMS
Metastable xenon Electrostatic thruster Collisional-radiative model
Relativistic Breit-Pauli b-spline matrix method

16. SECURITY CLASSIFICATION OF:			17. LIMITATION OF ABSTRACT	18. NUMBER OF PAGES	19a. NAME OF RESPONSIBLE PERSON
a. REPORT	b. ABSTRACT	c. THIS PAGE			Yu-hui Chiu
UNCL	UNCL	UNCL	UNL		19B. TELEPHONE NUMBER *(Include area code)*

Block 13 (continued)

**Department of Physics and Astronomy, Drake University, Des Moines, IA 50311

#Department of Physics, Indian Institute of Technology, Roorkee 247667, India

IOP PUBLISHING JOURNAL OF PHYSICS D: APPLIED PHYSICS

J. Phys. D: Appl. Phys. **42** (2009) 185203 (8pp) doi:10.1088/0022-3727/42/18/185203

Near-infrared collisional radiative model for Xe plasma electrostatic thrusters: the role of metastable atoms

Rainer A Dressler[1], Yu-hui Chiu[2], Oleg Zatsarinny[3], Klaus Bartschat[3], Rajesh Srivastava[4] and Lalita Sharma[4,5]

[1] Spectral Sciences Inc., 4 Fourth Ave, Burlington, MA 01803, USA
[2] Space Vehicles Directorate, Air Force Research Laboratory, Hanscom AFB, MA 01731, USA
[3] Department of Physics and Astronomy, Drake University, Des Moines, IA 50311, USA
[4] Department of Physics, Indian Institute of Technology, Roorkee 247667, India

Received 3 April 2009, in final form 6 July 2009
Published 24 August 2009
Online at stacks.iop.org/JPhysD/42/185203

Abstract

Mestastable Xe atoms play an important role in the collisional radiative processes of dense xenon plasmas, including those of electric thrusters for space vehicles. Recent measurements and calculations of electron-excitation processes out of the $5p^5 6s$ $J = 2$ metastable state ($1s_5$ state in Paschen notation) have allowed for the development of a collisional radiative model for Xe near-infrared (NIR) emissions based on the population of the metastable level through $2p–1s_5$ radiative transitions, and based on depopulation through electron-impact excitation. A modified plasma radiative model incorporating newly computed electron-impact excitation cross sections using both relativistic distorted wave and semi-relativistic Breit–Pauli B-Spline R-matrix methods is presented. The model applies to optically thin, low-density regions of the thruster plasma and is most accurate at electron temperatures below 10 eV. The model is tested on laboratory spectral measurements of the D55 TAL and BHT-200 Hall thruster plasma NIR radiation. The metastable neutral fraction is determined to rise from 0.1 to slightly above 1% as the electron temperature increases from ~2 to 10 eV, reaching a maximum around 15 eV. Electron temperatures derived with the modified model are approximately 20% lower than a previous version of the model that used an approximate approach to account for metastable population and line intensity enhancement.

1. Introduction

Electrostatic thrusters for space propulsion, such as Hall thrusters and ion thrusters, offer significant propellant mass savings over chemical spacecraft engines. The development of engines in new performance regimes requires extensive testing in ground-based facilities to optimize the efficiency of plasma generation and ion acceleration. Since xenon is the preferred propellant, these tests can be very costly. Traditionally, the plasma emanating from the engine is characterized with plasma probes. Probe measurements, however, are problematic because they locally perturb the plasma, and because they are generally not made to survive the high plasma densities and temperatures near the engine. A passive optical diagnostic provides a non-intrusive means to rapidly retrieve plasma parameters such as the electron temperature and plasma density profiles. The primary challenge of a quantitative passive optical diagnostic is the development of a collisional radiative model (CRM) that converts absolute or relative line emission intensities into plasma parameters such as the electron temperature. In the past, the development of CRMs for xenon propelled electrostatic thrusters has been hindered by the high neutral and ion energy level densities, and the lack of emission excitation cross sections.

Recently, Karabadzhak, Chiu and Dressler (KCD) [1] developed a CRM for Xe propelled Hall thrusters based on experimental emission excitation cross sections determined at single-collision conditions [2]. The measurements demonstrated that the optical spectrum depends markedly on electron temperature, and that ion collisions at energies typical for electrostatic thruster acceleration voltages produced spectra that differed significantly from those induced by

[5] Present address: Physikalisches Institut, Universität Heidelberg, D-69120 Heidelberg, Germany.

electrons. The model, designed to calculate the intensities of prominent 2p–1s (Paschen notation) near-infrared (NIR) transitions, greatly reduces the system of coupled excitation and de-excitation rate equations by applying experimental emission excitation cross sections that include emissions due to cascades from higher states. An important weakness of the CRM is an approximate method to account for metastable atom populations. Emission excitation cross sections for metastable atoms can be significantly higher than the corresponding cross sections for ground state atoms due to the much lower excitation energies. At the time of development of the CRM by Karabadzhak *et al*, no excitation cross sections for Xe metastable atoms were available. Steady-state densities of metastable atoms were estimated by assuming that they are populated via radiative transitions from higher states and depopulated by excitation to the same optically coupled states that have sizeable radiation branching ratios to a 1s state that is optically coupled to the ground state. The electron-impact excitation cross sections were assumed to be proportional to the upper-state degeneracies. The derived model did not depend on absolute cross sections and the thus estimated relative cross sections led to satisfactory reproduction of spectra observed from an anode layer thruster discharge and plume. Significant line intensity enhancements by metastable excitation were determined for those lines where the lower state is metastable.

Since the development of the KCD CRM [1], Jung *et al* [3] reported measurements of NIR emission excitation cross sections from the $1s_5$ metastable state. Meanwhile, accurate methods have been developed with which electron-impact excitation cross sections for metastable atoms can be computed. Recently, we calculated cross sections for excitation of the 1s ($5p^5 6s$) metastable states to other 1s states and 2p ($5p^5 6p$) and 3d ($5p^5 5d$) states using the semi-relativistic Breit–Pauli B-Spline *R*-matrix (BSR) method [4]. This approach produces accurate cross sections near the threshold. Additionally, we computed cross sections for metastable excitation to 1s, 2p and 3p states using the relativistic distorted wave (RDW) approach, which is accurate at intermediate and higher electron energies. In this paper, we incorporate the recently determined experimental and theoretical cross sections in the KCD model, thereby creating a new radiative model that quantitatively accounts for metastable atom populations. In section 2, we introduce the salient features of the new model. We also discuss the recent cross section calculations and measurements in terms of their integration in the model. The theoretical excitation cross section work will be published in detail elsewhere. In section 3, the performance of the model will be demonstrated through comparison with experimental data from ground-test measurements.

2. Collisional radiative model

2.1. Model modifications

The KCD model was developed to predict relative intensities of 11 NIR lines associated with $2p_i$ upper states of the neutral Xe atom (Xe I). An expanded view of the pertinent atomic

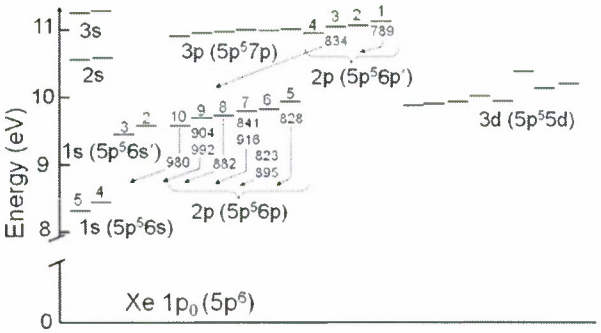

Figure 1. Schematic Xe I atomic energy level diagram highlighting the NIR transitions subject of the present CRM.

energy levels associated with these emission lines is shown in figure 1. Also shown are the transitions of interest and the respective wavelengths in nanometres. Given the very high radiative rates of the $2p_i - 1s_j$ transitions, the model can assume that the $2p_i$ states are depopulated only through radiative transitions, and not through electron collisional removal. Of the three $1s_j$ states that are associated with the intense NIR transitions, the $1s_5$ state is metastable with a lifetime of ~42 s [5]. Consequently, high excitation rates will lead to significant population of the $1s_5$ level, from which the $2p_i$ levels can be excited with significantly lower electron energies. According to Karabadzhak *et al* [1], the excitation rate of a particular NIR line at wavelength, λ, in energy units per steradian can then be expressed as

$$J_\lambda(\mathrm{Xe\,I}) = \frac{hc}{4\pi\lambda} N_0 N_e \left(k^\lambda_{c0} + \frac{N_m}{N_0} k^\lambda_{cm} + \alpha \cdot k^\lambda_1 + \frac{1-\alpha}{2} k^\lambda_2 \right), \tag{1}$$

where N_0 is the neutral atom number density, N_e is the electron number density, N_m is the metastable atom number density, $\alpha = N_1/N_e = N_1/(N_1 + 2N_2)$ is the ratio of singly charged ion density to the total ion density or electron number density, k^λ_{c0} is the ground-state atom electron-impact line emission excitation rate coefficient, k^λ_{cm} is the metastable-atom electron-impact line emission excitation rate coefficient and k^λ_1 and k^λ_2 are the singly and doubly charged ion collision emission excitation rate coefficients. As determined by Chiu *et al* [2] and Sommerville *et al* [6], absolute emission excitation rates due to ion collisions contribute significantly to the observed radiance at low electron temperatures. In equation (1), it is assumed that given the high ion energies at typical electrostatic thruster acceleration voltages, the difference between ion-induced ground-state atom and metastable atom emission excitation cross sections is not significant, and that excitation of ions by metastables can be neglected due to the much lower metastable densities in comparison with ground-state atom densities. The electron-temperature dependent rate coefficients are calculated through the usual means by convoluting the energy dependent cross sections with the collision velocity distribution [1]:

$$k_e(T) = \langle f(E_e)\sigma_e(E_e)v_e \rangle_T, \tag{2}$$

where E_e is the electron energy, $f(E_e)$ is the normalized electron energy distribution, $\sigma_e(E_e)$ is the electron energy

dependent excitation cross sections and v_e is the corresponding electron velocity. The model assumes a Maxwell–Boltzmann electron energy distribution. For ion-excitation rates, a delta-function at the nominal accelerated ion energy is assumed:

$$k_{\text{ion}}(E_{\text{ion}}) = \sigma_{\text{ion}}(E_{\text{ion}})(2E_{\text{ion}}/m_{\text{ion}})^{1/2}, \tag{3}$$

where m_{ion} is the atomic mass of the ion.

The steady-state rate equation for population and depopulation of the $1s_5$ metastable state can be written as

$$N_0 N_e \left(k_{0m} + \sum_i \left\{ k_{c0}^i + \alpha k_1^i + \frac{1-\alpha}{2} k_2^i \right\} \right) = N_m N_e \left(\sum_j P_j k_{2pm}^j + \sum_k k_{dm}^k + k_{\text{ion}} \right), \tag{4}$$

where on the right-hand side, representing depopulation rates, k_{2pm}^j are metastable excitation rate coefficients to the $2p_j$ levels, P_j are the corresponding branching ratios for radiation from the $2p_j$ level to the $1s_4$ state that is optically coupled to the ground state and k_{dm}^k are metastable excitation rate coefficients to other atomic level manifolds for which repopulation rates to the $1s_5$ state through radiative transitions can be neglected. The sum over j occurs for all upper states that are optically coupled to the ground state. The sum over k involves $1s_5$ excitation rates to all other levels such as other 1s states, and 3d and 3p levels. k_{ion} is the $1s_5$ electron-impact ionization rate coefficient. On the left hand side, representing population rate coefficients, k_{0m} is the direct excitation rate from the Xe ground state ($1s_0$). The sum on the left-hand side of equation (4) is over emission excitation rate coefficients for which the lower state is the $5p^5 6s$ $J = 2$ ($1s_5$) level [7]. While these line emission excitation rate coefficients include cascade contributions, the right-hand side of equation (4) neglects cascades. Both the present computations and the experiments by Jung *et al* [3] justify the neglect of cascade contributions for the rate coefficients in the terms on the right-hand side of equation (4) at the electron energies of interest.

Equation (4) makes two important assumptions. First, metastable loss due to diffusion is neglected. Karabadzhak *et al* estimated that this assumption is typically valid in the discharge of the engine and applies at electron temperatures exceeding 1.8 eV for plasma densities exceeding $10^{10}\,\text{cm}^{-3}$ [1]. Second, equation (4) implies that the $1s_5$ level is the only mestastable state to affect the observed spectrum. The $5p^5 6s$ $J = 0$ ($1s_3$) level associated with the $J = 1/2$ ionic core is also metastable and lies very close in energy to the $2p_i$ states associated with the $J = 3/2$ core. Thus, this level could also enhance emission intensities through electron-induced transitions to the respective $2p_i$ levels. Population of the $1s_3$ state, however, occurs through weak optical transitions associated with $J = 1/2$ core $2p_2$ and $2p_4$ levels, and the ground-state atom emission excitation cross sections of the respective lines have been determined to be at least an order of magnitude smaller than those associated with the other $2p_i$ levels [8]. Consequently, $1s_3$ metastable populations and associated enhancement of the present NIR lines should not be significant. Equation (4) can be rearranged to provide the steady-state metastastable atom fraction:

$$N_m/N_0 = \left(k_{0m} + \sum_i \left\{ k_{c0}^i + \alpha k_1^i + \frac{1-\alpha}{2} k_2^i \right\} \right) \times \left(\sum_j P_j k_{2pm}^j + \sum_k k_{dm}^k + k_{\text{ion}} \right)^{-1}. \tag{5}$$

During the development of the KCD model, electron-impact excitation cross sections necessary to compute rate coefficients k_{2pm}^j and k_{dm}^k were not available, and an approximate approach using relative excitation cross sections for $1s_5$–$2p_i$ transitions based on upper state degeneracies was applied. Assuming the application of optical selection rules, the k_{dm}^k term was neglected. Depopulation through ionization was also not considered, even though theoretical work on the respective cross sections already existed [9–11]. Since then, all necessary experimental and theoretical cross sections are available that permit the computation of absolute metastable fractions using equation (5), which subsequently can be inserted into equation (1) on a line-by-line basis.

2.2. *Cross section set*

This work is based on recent measurements [3] and calculations of crucial Xe $1s_5$ excitation cross sections. The calculations will be described and presented in detail in forthcoming publications. The present section is limited to comparing sample results and describing the integration of the cross sections in the CRM. The BSR calculations performed at Drake University produced cross sections for electron-impact excitation to all $1s_i$ ($i > 0$), 2p and 3d states from the ground and metastable $1s_3$ and $1s_5$ states at electron energies ranging from threshold to 72 eV. Srivastava and Sharma used the RDW approach [12]. Calculations were performed for excitation of $1s_3$ and $1s_5$ levels to $1s_i$ ($i > 0$), and all $2p_i$ and $3p_i$ levels. For $2p_j$ excitations from the ground state, we use previously published cross sections implemented in the original model [2], including ion collision excitation cross sections [6] more recently reported for a broader range of ion impact energies. The electron-impact cross sections have also been parametrized with respect to the pressure dependence caused by radiation trapping [8] using an empirical form introduced by Chiu *et al* [2]. To date, application of the cross sections to model Hall thruster plasmas have found that the zero-pressure extrapolated experimental cross sections produce the best agreement with experimental spectra, and we conclude that the investigated external regions of thruster plasma are optically thin. While no experimental values are obtained for direct ground-state excitation to the $1s_5$ state, we use BSR results for the $1s_0$–$1s_5$ direct excitation cross sections

Figure 2 exhibits the cross sections for $1s_5$–$2p_6$ and $1s_5$–$2p_8$ excitation that contribute to the prominent 823 and 882 nm lines. The experimental data by Jung *et al* [3] are compared with the BSR and RDW results. At low energies, the RDW cross sections exceed the BSR and experimental values considerably. This is not surprising since it is well established that RDW, being a perturbation method, loses its accuracy at

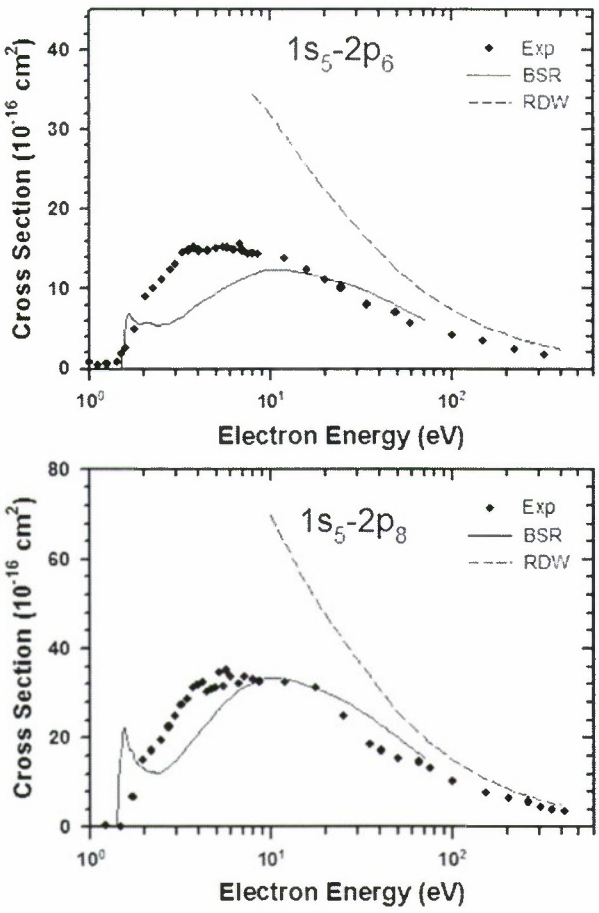

Figure 2. Comparison of experimental and computed electron-impact excitation cross sections as a function of electron energy for the $1s_5$–$2p_6$ (top frame) and $1s_5$–$2p_8$ (bottom frame) transitions. 'Exp' refers to the measurements of Jung *et al* [3], 'BSR' to the Breit–Pauli B-Spline *R*-matrix method, and 'RDW' to the relativistic distorted wave method.

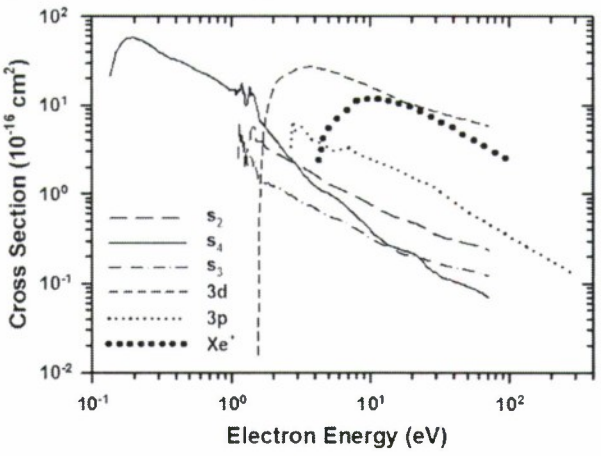

Figure 3. Electron energy dependence of $1s_5$ electron-impact excitation cross sections involving optically forbidden transitions. 3p and 3d refer to a sum of all $1s_5$ excitation cross sections to the respective $3l$ states. All cross sections are computed using the BSR method except for the 3p cross sections, where results from a previous semi-relativistic *R*-matrix calculation [13] are used at energies below 8 eV, and RDW values are used above 8 eV. Xe^+ refers to $1s_5$ metastable ionization cross sections by Ton-That and Flannery [11].

low electron energies. At the highest BSR energies, all three data sets are in much better agreement. At lower energies, the BSR cross sections are found to exhibit two maxima, one very near the threshold and the other one around ~10 eV. The threshold peak is not observed in the experiments. This can be explained by experimental broadening due to the electron energy resolution. The peak at higher energies appears at slightly lower electron energies in the experiments than in the BSR theory.

Figure 3 compares BSR results for electron-induced transitions from the $1s_5$ state to other $1s_i$ states, as well as the sum of all cross sections to the $3d_i$ states, designated as 3d. The figure also includes the sum of all cross sections to the $3p_i$ states (designated 3p). These cross sections were calculated using the RDW method above 8 eV. At lower energies, $1s_5$–3p cross sections are used that were calculated in an earlier study [13] using a different semi-relativistic Breit–Pauli *R*-matrix approach that, as a close-coupling method, unitarizes the *S* matrix. The $1s_5$–$1s_4$ cross sections are very large near the threshold due to the low excitation energy (0.12 eV). This transition, therefore, dominates the metastable depopulation at low electron temperatures. This is in contrast to assumptions made in the original CRM, where all depopulating transitions were postulated to occur through the optically allowed $1s_5$–$2p_i$ transitions. This implies that the KCD model overestimates the metastable population. The magnitude of the BSR 3d and RDW 3p excitation cross sections, in comparison with the $2p_i$ excitation cross sections at similar energies, suggest that these transitions have a growing effect on the metastable state population fraction with electron energy. Finally, $1s_5$ state ionization cross sections are shown that were taken from Born calculations by Ton-That and Flannery [11]. These values are similar to those computed by Hyman [10] and Deutsch *et al* [9]. We have chosen the cross sections by Ton-That and Flannery because they lie in between the other cross section sets.

The model calculations described in the next section use two sets of cross sections for comparison purposes and to assess the sensitivity of the model with respect to the cross sections. In the first, designated BSR-RDW, we use the BSR cross sections at energies below 70 eV, and the RDW cross sections at higher energies for the $1s_5$–$2p_i$ transitions. For the $1s_5$–$3d_i$ transitions, only BSR calculations are available. In the second set, designated BSR-RDW-Jung, we replace the BSR $1s_5$–$2p_i$ cross sections with the experimental data of Jung *et al* [3]. The model is used to extract electron temperatures from two Hall thrusters, the TSNIIMASH 1.35 kW D-55 anode layer thruster (TAL) and the Busek Inc. 200 W BHT-200 engine.

3. Results and discussion

3.1. D-55 TAL

The spectral data used in the present analysis were previously reported by Karabadzhak *et al* [1]. The D-55 TAL has an acceleration voltage of 300 V. For all of the calculations we

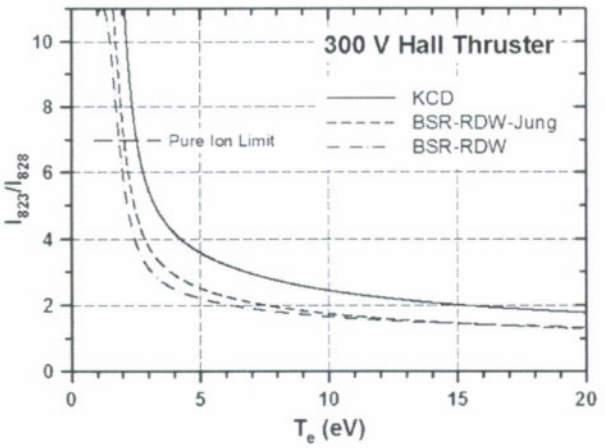

Figure 4. 823 and 828 nm line intensity ratios as a function of electron temperature computed for a 300 V acceleration voltage Hall thruster using the KCD (original) and present model incorporating the BSR-RDW-Jung and BSR-RDW cross sections sets (see table 1 caption for explanation). 'Pure ion limit' refers to the low temperature limit where only ion excitation leads to radiance.

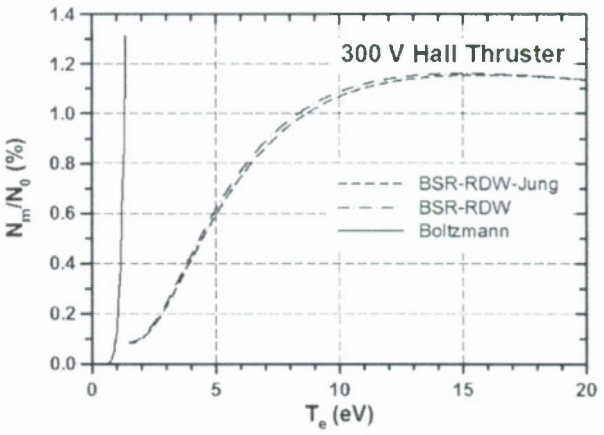

Figure 5. Steady-state metastable population fraction, N_m/N_0, as a function of electron temperature.

assumed a charge fraction, $\alpha = 0.8$, and an ion energy of 250 eV per charge, the latter value computed by Boyd [14]. Figure 4 compares the 823/828 nm intensity ratios as a function of electron temperature computed using the original KCD model and the presently modified CRM using the two sets of cross sections, BSR-RDW and BSR-RDW-Jung, introduced in the previous section. The intensity ratio between the 823.2 and 828.0 nm lines offers a rapid and reliable means for determining the local electron temperature of a Hall thruster plasma. The 823 nm and 828 nm lines are associated with the $2p_6$–$1s_5$ and $2p_5$–$1s_4$ transitions, respectively (see figure 1). Electron-impact excitation of the $1s_5$ metastable state to the optically forbidden $2p_5$ level is significantly less efficient in comparison with the optically allowed $2p_6$ level [3]. The 823/828 nm intensity ratio is, therefore, very sensitive to $1s_5$ excitation cross sections and the $1s_5$ population.

The horizontal dashed line in figure 4 labelled 'pure ion limit' represents the low electron temperature limit where only ion excitation leads to radiance. The original CRM crosses this limit at ~2.6 eV, while the computations with the purely and partially theoretical metastable excitation cross sections cross it at 2.1 eV and 1.9 eV, respectively. As mentioned earlier, the present CRM neglects metastable atom diffusion losses, which are expected to become important at electron temperatures below ~1.8 eV at densities below 10^{10} cm^{-3} [1]. The presently modified CRM approaches the pure ion limit very near where the model becomes inaccurate. The present calculations determine that approximately 40% of the NIR radiance is attributable to ion-excitation processes at 1.8 eV. It is, therefore, conceivable that the intensity ratio reaches a maximum prior to approaching the pure ion limit as the electron temperature is decreased.

The figure demonstrates that the presently modified CRM produces lower intensity ratios than the KCD model. This confirms that the additional metastable depopulation mechanisms included in the present models have an important effect in the extracted electron temperature. The substantially higher metastable enhancement in the KCD model can be additionally attributed to the fact that it only considers relative $1s_5$–$2p_i$ cross sections and does not take into account the threshold behaviour, thereby leading to inaccuracies at low electron temperatures. The relative metastable excitation cross sections of the original CRM did not allow for a quantification of the $1s_5$ state population ratio, N_m/N_0. In the present model, the inclusion of absolute cross sections allows for the computation of this steady-state population fraction through equation (5). Figure 5 compares the electron temperature dependence of this ratio for the two sets of metastable excitation cross sections used in figure 4. The metastable population fraction increases with electron temperature to a maximum value of ~1.16% at an electron temperature of ~15 eV. Figure 5 demonstrates that the metastable atom density is very sensitive to the electron temperature in the critical 2–10 eV region. The calculated ratios for the two sets of cross sections are very similar, suggesting that the more significant differences in 823/828 intensity ratios observed for the two cross section sets is mainly due to the differences in the experimental and computed $1s_5$–$2p_6$ emission excitation cross sections. From the comparison of Jung and BSR cross sections shown in figure 2 it can be concluded that the excitation rates will be significantly higher using the experimental data by Jung *et al* at low electron temperatures.

In figure 5, we also compare the metastable population ratio derived from an equilibrium Boltzmann distribution:

$$\frac{N_m}{N_0} = g_m \exp(-E_m/kT_e), \tag{6}$$

where g_m is the level degeneracy ($g_{1s5} = 5$) and $E_m = 8.315$ eV is the level energy with respect to the ground state. The significantly higher equilibrium population ratio emphasizes the inappropriateness of an equilibrium treatment. Equilibrium approaches have been used to derive total neutral densities from laser probes of $1s_5$ population densities [15, 16].

Figure 6 shows model spectral fits to a TAL chamber measurement [1] collected from an axial point that was 200 mm

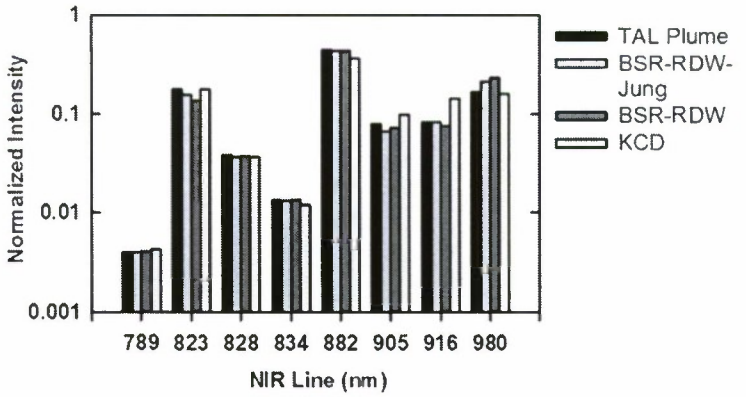

Figure 6. Spectral intensities observed in the plume of a D-55 TAL thruster (TAL) compared with intensities modelled using the KCD model and the present model using the BSR-RDW-Jung and BSR-RDW cross sections sets.

Table 1. CRM results obtained from modelling NIR spectral intensities at 200 and 25 mm from the exit plane of a 300 V anode layer thruster. KCD refers to the CRM of Karabadzhak *et al* [1], BSR-RDW-Jung to the presently upgraded model using computed metastable excitation cross sections and experimental $1s_5$–$2p_i$ cross sections computed by Jung *et al* [3] and BSR-RDW refers to mestastable excitation using only computed $1s_5$ excitation cross sections (see text for details). 823/828 and 834/828 refer to a 2-line analysis based on the respective intensity ratios (figure 4). 8-line analysis refers to a best fit to the intensities at the eight wavelengths shown in figure 6. χ is the standard deviation of the 8-line analysis.

	T_e (eV)			
	823/828	834/828	8-line	χ
		200 mm		
KCD	3.4	2.8	3.4	0.284
BSR-RDW-Jung	2.5	2.8	2.7	0.124
BSR-RDW	2.3	2.8	2.6	0.176
		25 mm		
KCD	5.6	4.8	6.1	0.318
BSR-RDW-Jung	3.4	4.8	4.5	0.252
BSR-RDW	2.8	4.8	4.6	0.302

from the exit plane of the engine. Eight independent (different $2p_i$ upper states) NIR emission lines were chosen for the fit. The intensities are normalized and are shown on a logarithmic scale. The presently modelled spectral intensities exhibit a markedly improved comparison with experiment at the higher wavelengths of 882, 904 and 916 nm, while the KCD model provides a better agreement at 823 nm. Interestingly, a first upgrade of the KCD model consisting of introducing only the experimental $1s_5$–$2p_i$ excitation cross sections resulted in a complete failure of the model in reproducing the observed spectra assuming reasonable electron temperatures. This emphasizes the importance of adding the de-excitation processes, $1s_5$–$1s_i$, $1s_5$–$3p_i$ and $1s_5$–$3d_i$, and $1s_5$–Xe^+, for which only theoretical cross sections are available.

Table 1 summarizes the electron temperatures extracted from the TAL results using the different models and cross sections sets. The models were also applied to a spectrum recorded in a higher electron-temperature region just 25 mm from the discharge channel exit plane (off axis). The results are shown for both a 2-line and 8-line electron-temperature extraction. For the 8-line analysis, the 789, 823, 828, 834, 882, 904, 916 and 980 nm were chosen as they are all from unique 2p levels. Following least-squares sum, χ^2, was minimized:

$$\chi^2 = \frac{1}{n}\sum_{i=1}^{n}\frac{(I_i^{\exp} - I_i^{\mathrm{CRM}})^2}{(I_i^{\exp})^2}, \qquad \sum_{i=1}^{n} I_i^{\exp} = \sum_{i=1}^{n} I_i^{\mathrm{CRM}} = 1. \tag{7}$$

Here n is the number of lines, while $I_i^{\exp}$ and I_i^{CRM} are the normalized experimental and best-fit modelled line intensities. In addition to the 823/828 nm intensity ratio, we show results extracted for the 834/828 nm ratio, where both wavelengths are associated with transitions that involve a lower state that is optically coupled to the ground state. Consequently, that particular ratio is unaffected by the choice of metastable excitation model.

Of the three models listed in table 1, the present model using the BSR-RDW-Jung cross section set exhibits the best performance in terms of the lowest standard deviation, and in terms of the best agreement between the three temperature extractions. The 200 mm electron temperatures retrieved using the BSR-RDW cross section set do not deviate substantially from the BSR-RDW-Jung set, however, the 8-line and 823/828 extractions are more than 0.6 eV lower than the KCD results. Karabadzhak *et al* [1] report for the same TAL experimental setup an electron temperature of 3.0 eV, which was recorded with a Langmuir probe at an axial distance of 300 mm. This value lies 0.3 eV higher than the present model using the BSR-RDW-Jung cross section set.

Applying the models to a spectrum recorded at 25 mm from the exit plane results in significantly higher standard deviations as well as larger differences between the various extraction methods. For the present models, the temperature extracted from the 823/828 ratios are significantly lower than the 8-line and 834/828 ratio extractions. As already seen in figure 6, the present models somewhat underestimate the 823 nm line intensity in the fit to the eight lines, hence suggesting that errors may exist in the cross sections used for

excitation of this line. As seen in figure 4, the 823/828 nm ratio is seen to level off above 3 eV, thereby leading to a reduction in the accuracy of the electron-temperature extraction. This effect is most severe for the entirely theoretical set (BSR-RDW) of metastable excitation cross sections.

The data in table 1 may lead to the conclusion that the 834/828 nm ratio, which is minimally affected by metastables, provides the most accurate extraction of the electron temperatures. As already pointed out by Karabadzhak *et al*, the 834.7 nm line intensity is very weak (approximately one third of the 828.2 nm line, see figure 6) and requires a high-resolution spectrograph to avoid interference from other lines. Weaker Xe I lines lie within 0.06 and 0.3 nm of the primary Xe I line. More problematic is a Xe II line that lies within 0.05 nm of the main 834.7 nm line. This ionic line involves relatively low-lying states of the ion and its emission intensity is expected to increase with electron temperature. Nevertheless, the excellent comparison between the 8-line analysis and the 834/828 extraction at low electron temperatures is very satisfying, particularly when considering that the experimental data were very carefully recorded for this case [1].

As already pointed out by Karabadzhak *et al* [1], the model loses accuracy at the elevated electron temperatures and higher electron densities of the discharge. This problem is not alleviated by the present rendition of the model. A comparison with discharge spectra predicted electron temperatures exceeding 70 eV. We noticed that the 881.9 and 980.0 nm lines are significantly overestimated in the model, thus suggesting either a problem with the cross sections or that highly non-Boltzmann electron energy distributions are at play. At the highest densities in the discharge channel of a Hall thruster, the assumption that the $2p_i$ states, as well as the 3p and 3d levels, are only depopulated through radiative transitions, is no longer valid.

3.2. *BHT-200 Hall thruster*

Matlock and coworkers recently reported an optical analysis of the 200 W BHT-200 Hall thruster based purely on the 823/828 nm line ratio [17]. This engine operates optimally with a 250 V acceleration potential. Figure 7 displays the modelled ratio curves as a function of electron temperature for the three variants of the CRM used earlier assuming ion energies of 200 eV per charge. Only minor differences with the curves presented in figure 4 are noticeable below electron temperatures of 3 eV, where ion cross sections are important. The ion excitation cross sections decline with decreasing ion energy, as reported by Sommerville *et al* [6]. The ion energy dependence of the ion collision excitation cross sections is most noticeable in the decline of the pure ion limit shown in figure 7 in comparison with the 300 V system (figure 4). The computations also produced metastable population ratios very similar to those determined for the 300 V Hall thruster system modelled in section 3.1.

Table 2 compares the extracted electron temperatures for a series of intensity ratio measurements reported by Matlock *et al* [17] as a function of radial distance with respect to

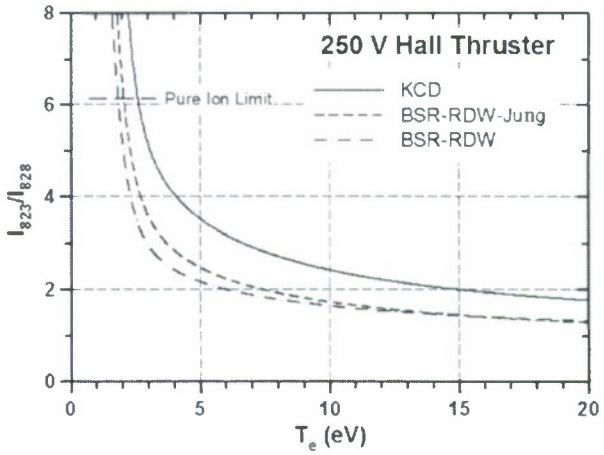

Figure 7. 823 and 828 nm line intensity ratios as a function of electron temperature computed for a 250 V acceleration voltage Hall thruster using the KCD (original) and present model incorporating the BSR-RDW-Jung and BSR-RDW cross sections sets (see table 1 caption for explanation). 'Pure ion limit' refers to the low temperature limit where only ion excitation leads to radiance.

Table 2. Modelled electron temperatures (eV) extracted from 823/828 nm intensity ratios [17] recorded from the BHT-200 engine along a radial profile at a distance of 8 mm from the thruster exit plane. The radial distance, r, is tabulated in units of the annulus outer diameter (OD = 3.2 cm). Models KCD, BSR-RDW-Jung and BSR-RDW are the same as defined in table 1.

r (OD)	I_{823}/I_{828} (Exp) [17]	BSR-RDW-Jung	BSR-RDW	KCD
0	4.66	2.4	2.2	3.3
0.07	4.80	2.4	2.1	3.2
0.13	5.05	2.3	2.1	3.1
0.19	5.10	2.3	2.1	3.0
0.25	4.18	2.6	2.3	3.8
0.32	4.66	2.4	2.2	3.3
0.38	5.21	2.3	2.0	3.0
0.44	5.70	2.2	1.9	2.8
0.5	6.82	2.0	1.8	2.5
0.56	7.00	2.0	1.8	2.4
0.63	6.01	2.1	1.9	2.7

the thruster axis. The radial profile was conducted 8 mm from the thruster exit plane. As in the TAL comparison, the extracted electron temperatures of the models using absolute metastable excitation cross sections are lower than those of the KCD model. Langmuir-probe measurements on the BHT-200 thruster have not been reported for axial distances less than 50 mm. At that distance, Beal and coworkers [18] report an axial electron temperature of 2.6 eV. This value agrees closely with calculations conducted using a particle-fluid hybrid approach [19]. That same model predicts an electron temperature of ~3.9 eV at an axial distance of 8 mm. The model, however, did not take into account that the BHT-200 has a central nosecone that protrudes approximately 7 mm from the exit plane, and is likely to perturb the plasma. Matlock *et al* reported computations using a hybrid particle-in-cell model, HP Hall, that models the discharge and channel with an accurate description of its geometry [17]. The HP-Hall

prediction of an electron temperature of 2 ± 1 eV near the nosecone is fully consistent with the present optical analysis near the thruster axis.

4. Conclusions

We introduce an improved Xe electrostatic thruster CRM that overcomes the main weakness of the KCD CRM by incorporating both experimental and theoretical absolute electron-impact excitation cross sections associated with the $1s_5$ metastable population and depopulation rates. A markedly improved performance of the CRM is found when incorporating BSR and RDW cross sections for all $1s_5$ related electron-induced processes, except for the $1s_5$–$2p_i$ transitions, for which experimental data by Jung *et al* [3] were used. The performance is measured in terms of a lower standard deviation in reproducing relative, normalized spectral line intensities for independent NIR emission lines, and an improved comparison between electron-temperature extractions using multi-line and 2-line approaches. The model demonstrates that the original KCD model overestimates the metastable populations due to the neglect of important, optically forbidden and ionization depopulation processes. For both engines modelled in this paper, mestastable population fractions, N_m/N_0, ranging between 0.1 and ~1.2% are predicted at electron temperatures ranging between 2 and 20 eV.

The improved performance of this upgraded CRM, that quantitatively accounts for metasable population fractions, suggests that it can also be applied to analysing absolute emission line intensities in order to non-intrusively extract plasma densities. This could be accomplished by applying tomographic approaches such as the one introduced by Matlock *et al* [17].

Acknowledgments

This work is supported by the US Air Force Office of Scientific Research under tasks 2301HS and 2303EP02 (Program Managers: Kent Miller and Michael R Berman). OZ and KB acknowledge grant support, in part, by the United States National Science Foundation (Grant Nos PHY-0555226 and PHY-0757755). RS acknowledges the support of the Asian Office of Aerospace Research Development, Tokyo, Japan (Grant No 064029). The authors are grateful for very helpful suggestions by the referees, in particular the recommendation by one to include ionization rates in equation (4).

References

[1] Karabadzhak G F, Chiu Y and Dressler R A 2006 *J. Appl. Phys.* **99** 113305
[2] Chiu Y, Austin B L, Williams S, Dressler R A and Karabadzhak G F 2006 *J. Appl. Phys.* **99** 113304
[3] Jung R O, Stone T E, Boffard J B, Anderson L W and Lin C C 2005 *Phys. Rev.* A 72 022723
[4] Allan M, Zatsarinny O and Bartschat K 2006 *Phys. Rev.* A **74** 030701
[5] Walhout M, Witte A and Rolston S L 1994 *Phys. Rev. Lett.* 72 2843
[6] Sommerville J D, King L B, Chiu Y and Dressler R A 2008 *J. Propulsion Power* **24** 880
[7] Radzig A A and Smirnov B M 1985 *Reference Data on Atoms, Molecules, and Ions* ed J P Toennies (Berlin: Springer)
[8] Fons J T and Lin C C 1998 *Phys. Rev.* A **58** 4603
[9] Deutsch H, Becker K, Matt S and Mark T D 1999 *J. Phys. B: At. Mol. Opt. Phys.* **32** 4249
[10] Hyman H A 1979 *Phys. Rev.* A **20** 855
[11] Ton-That D and Flannery M R 1977 *Phys. Rev.* A **15** 517
[12] Srivastava R Stauffer A D and Sharma L 2006 *Phys. Rev.* A **74** 012715
[13] Petrov G M, Giuliani J L, Apruzese J P, Dasgupta A, Petrova T, Bartschat K and Rose D 2007 *J. Phys. D: Appl. Phys.* **40** 4532
[14] Boyd I D 2000 *J. Propulsion Power* **16** 902
[15] Yokota S, Matsui M, Sako D, Yamamoto N, Koizumi H, Komurasaki K, Nakashima H and Arakawa Y 2006 *42nd AIAA/ASME/SAE/ASEE Joint Propulsion Conf. and Exhibit (Sacramento, CA, 9–12 July) AIAA* 2006-5028
[16] Matsui M, Yokota S, Sako D, Komurasaki K and Arakawa Y 2007 *43rd AIAA/ASME/SAE/ASEE Joint Propulsion Conf. and Exhibit (Cincinnati, OH, 8–11 July) AIAA* 2007-5306
[17] Matlock T S, Hargus W A, Larson C W and Nakles M R 2007 *43rd AIAA/ASME/SAE/ASEE Joint Propulsion Conf. and Exhibit (Cincinnati, OH, 8–11 July) AIAA* 2007-5303
[18] Beal B E, Gallimore A D and Hargus W A 2003 *39th AIAA/ASME/SAE/ASEE Joint Propulsion Conf. and Exhibit (Huntsville, AL, 20–23 July) AIAA* 2003-5155
[19] Boyd I D and Yim J T 2004 *J. Appl. Phys.* **95** 4575